J. Membrane Biol. 166, 101–110 (1998)

The Journal of
Membrane
Biology

The Calculation of Intracellular Ion Concentrations and Membrane Potential from Cell-attached and Excised Patch Measurements. Cytosolic K^+ Concentration and Membrane Potential in *Vicia faba* Guard Cells

H. Miedema*, S.M. Assmann
Biology Department, The Pennsylvania State University, 208 Mueller Laboratory, University Park, PA 16802, USA

Received: 3 April 1998/Revised: 6 August 1998

Abstract. Ion channel activity in cell-attached patch recordings shows channel behavior under more physiological conditions than whole-cell and excised patch measurements. Yet the analysis of cell-attached patch measurements is complicated by the fact that the system is ill defined with respect to the intracellular ion activities and the electrical potential actually experienced by the membrane patch. Therefore, of the several patch-clamp configurations, the information that is obtained from cell-attached patch measurements is the most ambiguous. The present study aims to achieve a better understanding of cell-attached patch measurements. Here we describe a method to calculate the intracellular ion concentration and membrane potential prevailing during cell-attached patch recording. The first step is an analysis of the importance of the input resistance of the intact cell on the cell-attached patch measurement. The second step, and actual calculation, is based on comparison of the single channel conductance and reversal potential in the cell-attached patch and excised patch configurations. The method is demonstrated with measurements of membrane potential and cytosolic K^+ concentrations in *Vicia faba* guard cells. The approach described here provides an attractive alternative to the measurement of cytosolic ion concentrations with fluorescent probes or microelectrodes.

Key words: Intracellular ion concentration — Membrane potential — Cell-attached patch — K^+ channel — Stomata — *Vicia faba*

* *Present address:* Instituto de Biotecnologia, UNAM, Apartado Postal 510-3, Colonia Miraval, Cuernavaca, Morelos, Mexico, 62271

Correspondence to: S.M. Assmann

Introduction

In the cell-attached patch (CAP) configuration of the patch-clamp technique, the electrode is sealed onto a patch of membrane that remains part of the intact cell. Consequently, two membranes (the patch membrane and the rest of the cell membrane) intervene between the patch electrode and the bath electrode. This configuration results in two complications that hinder the interpretation of the resultant electrophysiological measurements. First, the pipette potential (V_p) is defined with respect to the potential of the reference electrode in the bath solution. Therefore, the resistance of the ion channel (R_c) in the patch and the membrane resistance of the intact cell, or cell input resistance (R_o), are situated in a voltage divider (Fig. 1). Consequently, at a given V_p, the actual voltage drop across the membrane patch depends on the ratio of R_o and R_c and the number of open channels. Second, the potential experienced by the patch membrane depends not only on V_p but also on the membrane potential of the intact cell (V_i), and the latter not only remains unknown but can change significantly during the CAP measurement, due to a net current through R_c in or out of the cell. With a change in V_i, the driving force for ion movement will change and as a consequence the measured single channel conductance in CAP ($g_{c,cap}$) will change as well. The measured reversal potential of the channel in the CAP configuration will also be affected. Both of these problems especially arise in relatively small cells, in which R_o may be of the same order of magnitude as R_c. In addition to R_c, the cell-attached membrane patch will have a background leak (R_p) caused by the presence of any other pathways for ion flow across the membrane. R_p has a similar effect on V_i as R_c. As is the case for R_c, the significance of R_p depends on its value relative to R_o rather than on its absolute value. The role of R_o/R_c and R_o/R_p in CAP

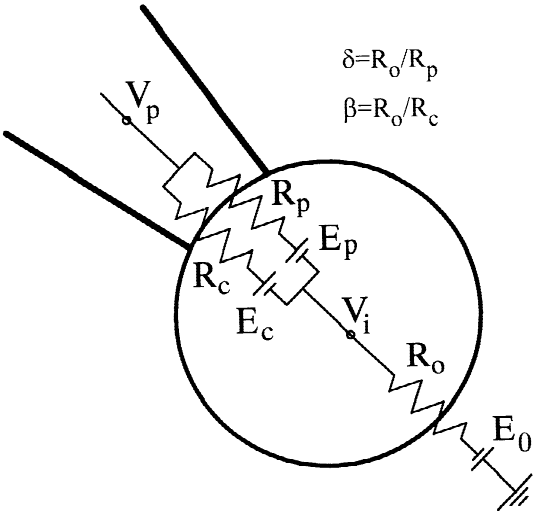

Fig. 1. Schematic representation of the cell-attached patch configuration, showing that the resistance of the ion channel in the patch (R_c) and the resistance of the background leak of the patch membrane (R_p) are positioned in series with the resistance of the intact cell membrane (R_o). Pipette and cell potential are indicated by V_p and V_i, respectively. In general, β equals NR_o/R_c, where N is the number of channels in the patch membrane. Note that the seal resistance is not indicated because it is an irrelevant resistance in the context of this paper (*see* text).

measurements has been the subject of several papers (Fischmeister, Ayer & DeHaan, 1986; Lynch & Barry, 1989; Barry & Lynch, 1991; Ravesloot et al., 1994).

The first step in the interpretation of CAP measurements is, thus, an understanding of the role of R_o. One way to achieve this is to study $g_{c,cap}$ in a patch containing more than one channel. As more channels open, a high R_o will result in a decrease of $g_{c,cap}$. On the other hand, a $g_{c,cap}$ that does not change with the number of open channels, and rectangular shaped current transients (Barry & Lynch, 1991) indicate that $R_o \ll R_c$ and $R_o \ll R_p$. Given that R_o/R_c and R_o/R_p are small, we provide a method to calculate the cytosolic ion concentration of the permeant ion species and from this the membrane potential as well. The method can be applied to both animal and plant cells and is exemplified here by measurements of the K^+ selective outward rectifier in the plasma membrane of *Vicia faba* guard cells (Miedema & Assmann, 1996), enabling calculation of the cytosolic K^+ concentration in this cell type (MacRobbie, 1988).

With the exception of calcium and pH probes, the use of ion selective probes in living cells is still in its infancy. The method described here allows calculation of the intracellular ion concentration for a variety of ionic species. In addition, the noninvasive nature of the method may be an advantage over, for instance, the use of ion selective microelectrodes. Another advantage of our method is that it also provides the membrane potential of the intact cell. Knowledge of the intracellular ionic conditions and membrane potential allows a valid comparison of ion channel characteristics obtained from cell-attached patch, excised patch, and whole-cell measurements.

Material and Methods

Plant Material and Protoplast Isolation

Plants of *Vicia faba* were grown and guard cell protoplasts were isolated as previously described (Miedema & Assmann, 1996). After isolation, the protoplasts were kept on ice and in the dark for two hours in a solution containing (in mM): 450 sorbitol, 0.5 $CaCl_2$, 0.5 $MgCl_2$, 0.5 ascorbic acid, 0.01 KH_2PO_4 and 5 MES, pH 5.5. For the K^+-uptake experiments, the procedure was the same but after isolation the cells were incubated on ice and in the dark in a solution containing 350 sorbitol, 50 KCl, 0.5 $CaCl_2$, 0.5 $MgCl_2$, 0.5 ascorbic acid, 0.01 KH_2PO_4 and 5 MES, pH 5.5. The average diameter of protoplasts used for the patch clamp experiments was 17 μm.

Patch-Clamp Measurements

The pipette solution always contained (in mM): 5 KCl, 5 K-Gluconate, 0.5 $CaCl_2$ and 10 Hepes, pH 7 (KOH). The CAP-bath solutions contained 1, 5 or 50 KCl, 5 K-Gluconate, 0.5 or 5 $CaCl_2$ and 10 Hepes, pH 7 (KOH). Where appropriate, potentials have been corrected for liquid junction potentials. For inside-out patch (IOP) measurements, the bath solution was exchanged for (in mM): 80 K-Gluconate, 2 EGTA with $CaCl_2$ added to give a final free Ca^{2+} concentration of 50 nM, 10 Hepes, pH 8 (KOH) and different amounts of KCl as indicated. Reversal potentials were corrected for ion activities and K^+ added by pH adjustment. Mannitol was added to all solutions to produce a final osmolality of 450 mmol kg^{-1}, except for the K^+-uptake experiments: CAP measurements on cells which were incubated in the 50 mM KCl solution were performed in a bath solution of osmolality 415 mmol kg^{-1}, because it proved extremely difficult to obtain GΩ seals in the regular 450 mmol kg^{-1} solution.

Measurements were performed using an Axopatch-1B patch-clamp amplifier and a DigiData 1200 Interface (both from Axon Instruments, Foster City, CA). The sampling rate was 5 kHz and currents were filtered at a −3 dB frequency of 1 kHz by the four-pole Bessel filter on the Axopatch-1B. Data analysis was accomplished using pCLAMP software (version 6.0.3, Axon Instruments). Membrane potentials and reversal potentials are defined as the potential at the cytosolic face of the membrane with respect to the potential at the external face of the membrane. Pipettes were pulled from Filamented Patch Clamp Glass (Catalog #5968, A-M Systems, Everett, WA). At the start of the experiment, the patch-clamp dish was filled with CAP-bath solution and the pipette resistance was between 80–100 MΩ (in the 5 mM KCl/ 5 mM K-Gluconate solution). After establishing an on-cell GΩ seal, typically 20 to 50 GΩ, and after pulling an IOP, the solution in the dish was replaced by IOP-bath solution. The experiments were performed under room light, resulting in a light intensity at the position of the patch clamp dish of <1 μE m^{-2} sec^{-1}.

Results

Theoretical Background

First we must address the possible impact of a high cell input resistance on cell-attached recordings. The quan-

titative analysis given here is based on the framework outlined by Barry and Lynch (1991). We suffice by giving the equations; readers who are interested in the derivations are referred to Barry and Lynch's excellent review. Where appropriate, the first number between parentheses refers to the corresponding equation in their paper. In contrast to Barry and Lynch's paper, our equations account for the number of open channels in the membrane patch, but describe steady-state current levels only.

When considering differences in current levels rather than absolute current magnitudes, the current through the seal resistance cancels out of the equations (Barry & Lynch, 1991). For this reason the seal resistance is absent from the following analysis. Before the patch pipette is sealed to the membrane, the cell or protoplast will be in a state of zero net current across its cell membrane and the membrane potential of the intact cell (V_i) will be given by its resting value E_0. After the establishment of a cell-attached seal, V_i is given by:

$$V_i = \frac{E_0 + V_p(\delta + N\beta) + E_p\delta + E_cN\beta}{1 + \delta + N\beta} \qquad \text{(A21, 1)}$$

where V_p is the pipette potential, E_c the diffusion potential of the channel, E_p the diffusion potential of the background leak, R_c the resistance of the channel, R_o the cell input resistance, R_p the resistance of the background leak, $\delta = R_o/R_p$, $\beta = R_o/R_c$. To account for the number of open channels in the patch (N), note that with respect to the original equation A21 in Barry and Lynch (1991) β has been replaced by $N\beta$. In extreme cases, R_p, R_c and R_o might be all of the same magnitude, implying values of δ and β close to unity (Barry & Lynch, 1991). However, even when δ and β are one order of magnitude lower than unity they will have a profound effect on the CAP measurement. To demonstrate these effects we arbitrarily choose δ and β to be 0.1. Figure 2*A* shows a simulation of $V_i - E_0$, i.e., the deviation of V_i from E_0, as a function of V_p. Equation 1 means that even before the channels of interest open ($\beta = 0$), a current through R_p may already change V_i. After channel opening, R_c provides an additional pathway for ion flow and V_i may change even more. Only in those cases where $R_o \ll R_p$ and $R_o \ll R_c/N$, i.e., when $\delta = \beta \approx 0$, does V_i remain unaffected and at E_0.

During a CAP measurement, the difference in steady-state current level (Δi_{tot}) before and after channels open is given by:

$$\Delta i_{tot} = N\, g_c \frac{E_0 - V_p + E_p\delta - E_c(1+\delta)}{(1+\delta)(1+\delta+N\beta)} \qquad \text{(A20, 2)}$$

where $g_c = 1/R_c$. Figure 2*B* shows a simulation of Δi_{tot} for the first open channel ($N = 1$) as a function of V_p at different values of δ and β. As is obvious from the *IV*-plots in Fig. 2*B*, the apparent or measured conductance in the CAP configuration ($g_{c,cap}$) depends on the values of δ and β. For the first open channel, the relationship be-

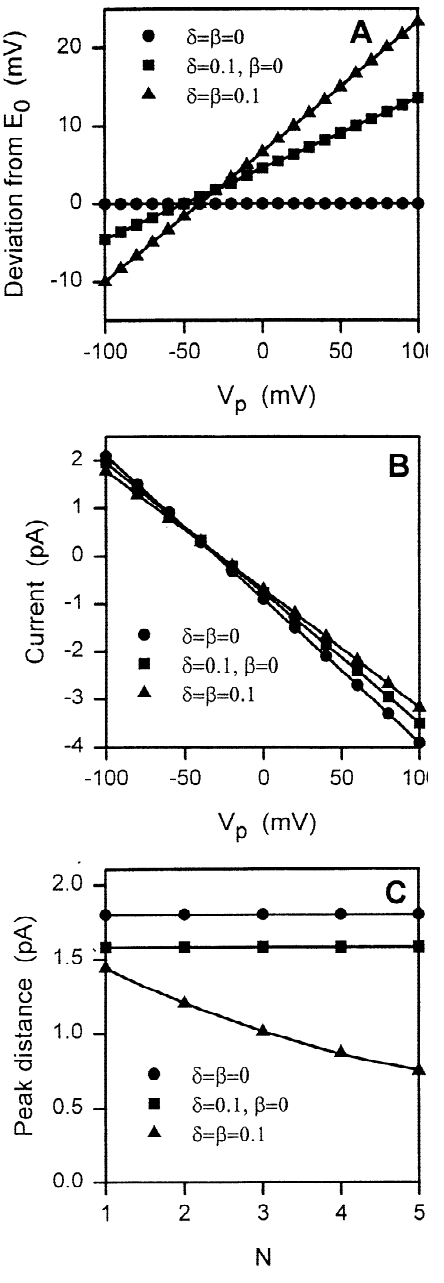

Fig. 2. (*A*) Simulation of the deviation of V_i from E_o (V_i-E_o) at different V_p and for different values of δ and β (*see* Eq. 1) (*B*) Simulated *IV*-curves for the first open channel ($N = 1$) in a patch studied in the CAP configuration, according to Eq. 2 and at different values of δ and β. (*C*) Simulation of the difference in current level between N+1 and N open channels, calculated at a V_p of 30 mV. For all calculations in (*A*), (*B*) and (*C*) the following parameter values were used: $E_c = -20$ mV, $E_o = -50$ mV, $E_p = 0$ mV, $g_c = 30$ pS.

tween the true single channel conductance (g_c) and $g_{c,cap}$ is given by:

$$g_c = (1 + \delta)(1 + \delta + \beta)g_{c,cap} \qquad \text{(A41, 3)}$$

Equation 3 means that whenever δ and β are significantly greater than zero, $g_{c,cap}$ is an underestimation of g_c. Note that although δ and β affect Δi_{tot}, the relationship between Δi_{tot} and V_p remains linear. In contrast, the relationship between N and Δi_{tot} is linear only as long as $\beta \approx 0$. Instead of plotting Δi_{tot} *vs. N*, Fig. 2*C* shows the difference in current level between N and $N + 1$ open channels, in relation to δ and β. Whenever β is significantly greater than 0, the distance between the peaks of the all-points histogram decreases with N. In the example of Fig. 2*C* ($\delta = \beta = 0.1$), the distance between the peaks of the all-points histogram would decrease from 1.44 pA for the first open channel to 1.01 pA for the third to 0.75 pA for the fifth open channel. This is an important observation as it enables us to get an indication of the significance of β (and thus of δ, as both depend on R_o). All we have to do is either inspect the all-points histogram or plot Δi_{tot} as a function of N and find out how Δi_{tot} behaves as more channels open. A second numerical example can further clarify the effect of δ and β on Δi_{tot}. According to Eq. 2, at a given value of V_p, the ratio of current levels corresponding to two and one open channel is given by:

$$\frac{(\Delta i_{tot})_{N=2}}{(\Delta i_{tot})_{N=1}} = \frac{2(1 + \delta + \beta)}{1 + \delta + 2\beta} \qquad (4)$$

For $\delta = \beta \approx 0$, $(\Delta i_{tot})_{N=2}/(\Delta i_{tot})_{N=1} = 2$. Now suppose that δ and β are both > 0 and moreover are of the same magnitude. Then, Eq. 4 means that a δ of, for instance, 0.14 will already result in a $(\Delta i_{tot})_{N=2}/(\Delta i_{tot})_{N=1}$ of 1.8. This effect will be reflected in a 20% decrease of the distance between the current peaks for one and two open channels in the all-points histogram.

During a CAP measurement not only $g_{c,cap}$, but also the measured reversal or zero current potential (V_p^0) depends on δ, where V_p^0 is defined as the potential at which $\Delta i_{tot} = 0$. The relationship between V_p^0 and the true reversal potential of the channel (E_c) is given by:

$$V_p^0 = E_0 + E_p\delta - (1 + \delta)E_c \qquad \text{(A42, 5)}$$

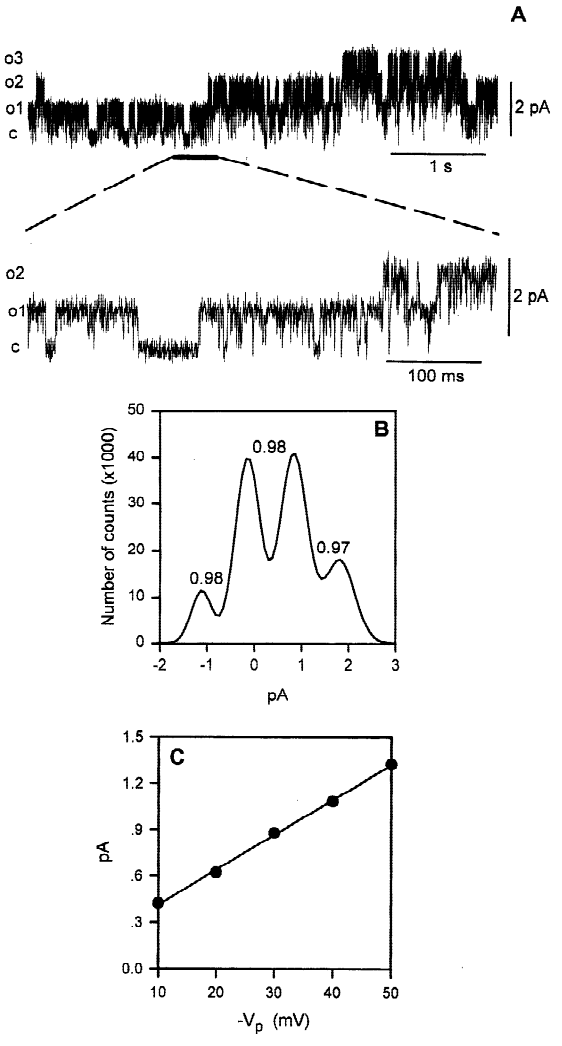

Fig. 3. (*A*) Example of a CAP recording of $I_{K,out}$ in *Vicia faba* guard cells, at a V_p of −40 mV and an external K^+ activity of 11 mM. Closing (*c*) and opening of one (o1) or more channels are indicated to the left of the traces. (*B*) All-points histogram based on a total recording time of 200 sec, including the 5-sec segment shown in (*A*). The solid line represents the fit using the Marquardt-Least Squares protocol in pClamp 6.0.3. Bin width = 0.08 pA. The distances (in pA) between fitted adjacent peaks are indicated. Note that the peak in the leftmost position represents the current level before channel opening and indicates a seal resistance of approximately 35 GΩ. (*C*) Relationship between the current magnitude and V_p of the channel shown in (*A*). Note that in order to assign outward current as positive, we plotted $-V_p$ instead of V_p.

Measurements on *Vicia faba*

Figure 3*A* shows a CAP recording of the K^+ selective outward rectifier ($I_{K,out}$) in the plasma membrane of *Vicia faba* guard cells. The rectangular shape of the current transients in Fig. 3*A* already indicates that the values of δ and β are relatively small. This expectation is confirmed by the equidistant peaks in the all-points histogram in Fig. 3*B*. We conclude that, in the case of this particular cell, $R_o \ll R_p$ and $R_o \ll R_c$. For approximately half of the over 54 *Vicia faba* guard cells studied, the observed decline in distances between the current peaks of the all-points histogram for, for instance, the first and the third open channel was 5–10%. For the other half of the cells, the decline fell typically between 10 and 20% and only very rarely as high as 20–30%. One reason that in about half of the cells studied, effects of δ and β on the

CAP measurement could safely be ignored is the size of the guard cells, here typically 17 μm. Especially for cells smaller than 15 μm one should expect to see effects of δ and β (Barry & Lynch, 1991). Interestingly, occasionally a 5–10% decrease in peak distance was observed in IOP recordings as well (*not shown*). Whatever the reason for this, it only strengthens our conclusion that in half of the *Vicia faba* guard cells we studied (those on which the analysis reported here is based) R_o was small, at least compared to R_c and R_p, and consequently did not interfere with the CAP measurement. Figure 3*C* shows the current magnitude in relation to V_p and demonstrates the Ohmic behavior of $I_{K,out}$ in the CAP configuration.

Figure 4*A* shows a recording of $I_{K,out}$ in an inside-out patch (IOP) and the corresponding all-points histogram is shown in Fig. 4*B*. IOP measurements can be considered as a limit case of CAP measurements with zero cell input resistance. In accordance with this, in most IOP recordings the distance between the peaks of the all-points histograms was indeed essentially constant. One reason to perform the excised patch measurement is to identify the ion selectivity of the channel. Figure 4*C* shows the relationship between the recorded reversal potential (E_{rev}) under different K^+ regimes and the Nernst potential of K^+ (E_K). As E_{rev} follows E_K closely we conclude that in the IOP configuration $I_{K,out}$ is selective for K^+. (In a previous paper (Miedema & Assmann, 1996) we erroneously concluded that $I_{K,out}$ shows some permeability for Cl^- as well).

When studied in the IOP configuration, $I_{K,out}$ totally inactivates at membrane potentials more negative than −20 to −30 mV (Miedema & Assmann, 1996). In the CAP configuration the channel also inactivated at hyperpolarized membrane potentials (*not shown*). A second remarkable feature of $I_{K,out}$ is the flickery open state current level (Figs. 3*A* and 4*A*). From the similarities in voltage sensitivity and flickering kinetics, we conclude that in both configurations one and the same channel has been studied. Consequently, it is assumed that in the CAP configuration, this channel shows a K^+ selectivity as well.

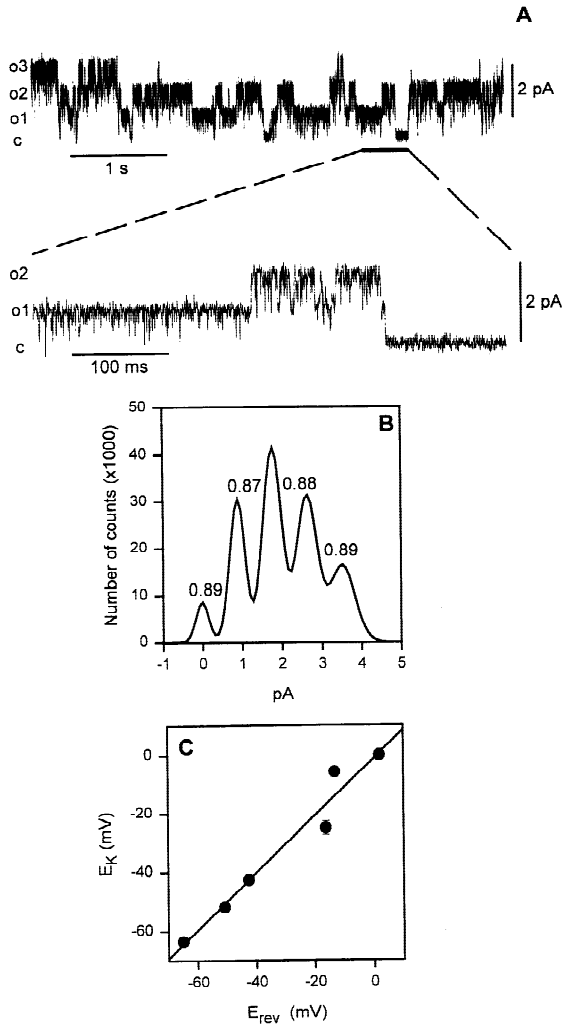

Fig. 4. (*A*) Current recording of $I_{K,out}$ in the IOP configuration at a membrane potential of 0 mV. Closing (*c*) and opening of one (o1) or more channels are indicated to the left of the traces. (*B*) All-points histogram based on a total recording time of 200 sec, including the 5-sec segment shown in (*A*). The solid line represents the fit using the Marquardt-Least Squares protocol in pClamp 6.0.3. Bin width = 0.08 pA. The distances (in pA) between fitted adjacent peaks are indicated. (*C*) Values of E_{rev} in the IOP configuration under different K^+ regimes in the bath as a function of E_K. Each data point (±SE) represents the average of at least six independent measurements. Where no error bars are indicated, SE was smaller than the symbol size.

Calculation of the Cytosolic Ion Activity

The starting point for the calculation of the cytosolic K^+ concentration is a mathematical expression that describes current flow through the channel in relation to voltage and to ion activities at both sides of the membrane during the IOP recording. The equation most commonly used is the Goldman-Hodgkin-Katz (GHK) current equation. However, from 36 *IV*-curves obtained from *Vicia faba* guard cells that we tried to fit to the GHK equation, only 13 could be fitted adequately by this equation. A typical example is shown in Fig. 5*A*. This figure shows three *IV*-plots obtained from one and the same IOP at different K^+ activities in the bath. As is obvious from Fig. 5*A*, the GHK equation cannot account for the observed currents for this particular channel type. An alternative current equation is given by Offner (1991):

$$I = g_c(E - E_c) \tag{6}$$

where g_c is given by:

$$g_c = P_s K_s \left(\frac{S_i}{S_i + K_s} + \frac{S_o}{S_o + K_s} \right) \tag{7}$$

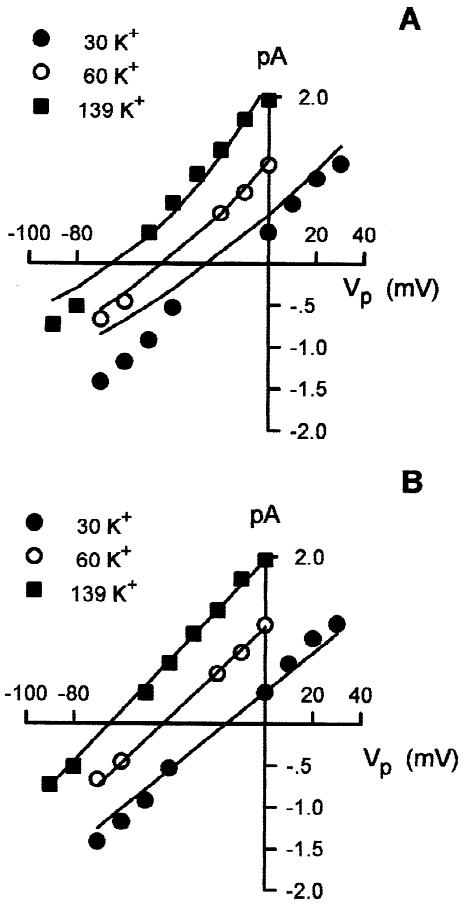

Fig. 5. (*A*) *IV*-plots obtained from IOP recordings of a single excised patch at different K^+ activities in the bath. The solid line represents the fit of the data to the GHK equation. (*B*) The same data as in (*A*) but now described with Eqs. 6 and 7 while using the values of K_s and P_s obtained from Fig. 6.

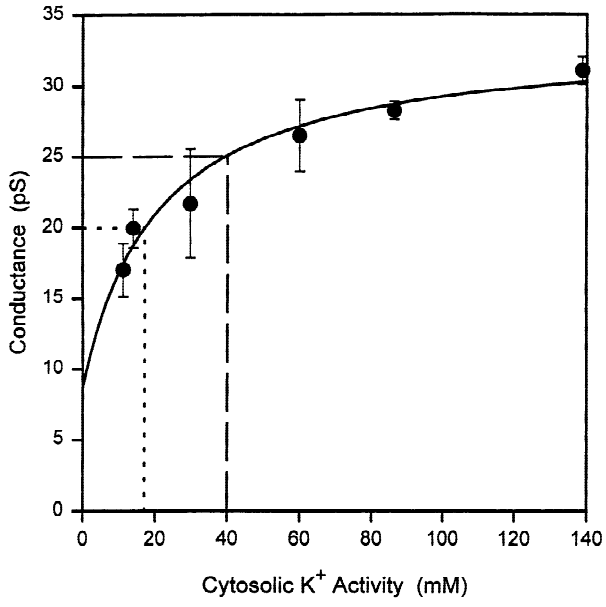

Fig. 6. The dependence of g_c on the K^+ activity at the cytosolic face of the membrane measured in the IOP configuration. The K^+ activity in the pipette was always 11 mM. The solid line represents the fit of the data points to Eq. 7, resulting in a K_s of 20 ± 2.8 mM and a P_s of 1.2 ± 0.11 pS/mM. Each data point is the average (±SE) of at least six independent measurements. The fit was employed with weight factors inversely proportional to SE. By interpolation, conductances of 20 and 25 pS indicate cytosolic K^+ activities of 17 and 40 mM, respectively (*see* text). K^+ activities given include the contribution of K^+ from KOH for pH adjustment.

and where P_s is a permeability coefficient, K_s the affinity of the channel binding site for its substrate, and S_i and S_o the internal and external ion activity, respectively. However, a direct fit of the data to Eqs. 6 and 7 proved to be extremely sensitive to the given starting values of P_s and K_s. Therefore we followed a different strategy and calculated P_s and K_s of $I_{K,out}$ from Fig. 6, which shows the empirical dependence of g_c on the K^+ activity on the cytosolic side of the membrane. A fit of the data in Fig. 6 to Eq. 7 resulted in a P_s of 1.2 ± 0.11 pS/mM and a K_s of 20 ± 2.8 mM. Note that the fit in Fig. 6 does not intercept the abscissa at zero pS. This is a consequence of Eq. 7 and means that at zero cytosolic K^+ ($S_i = 0$) g_c is exclusively carried by inward current. Although the channel may not mediate inward current under in vivo conditions, inward currents through these channels are clearly evident in tail current recordings (e.g., Miedema & Assmann, 1996). Figure 5*B* shows the same data as Fig. 5*A*, but now the solid lines represent calculated current magnitudes according to Eqs. 6 and 7 with the P_s and K_s values obtained from Fig. 6. We conclude that Offner's equation describes our data much better than the GHK equation.

Once we have the data to construct the plot in Fig. 6, the intracellular ion activity can be obtained by simple interpolation. Such an interpolation is valid because we previously ruled out effects of R_o on $g_{c,cap}$. Consequently, differences between g_c and $g_{c,cap}$ can only be ascribed to differences in ionic activities during the measurements. The only restriction is that both g_c and $g_{c,cap}$ must show Ohmic behavior (*see* Figs. 3*C* and 5). This is an essential condition because as long as V_i is unknown, comparison of g_c and $g_{c,cap}$ at exactly the same potential remains impossible. In the CAP configuration and at an extracellular (pipette) K^+ activity of 11 mM we measured a $g_{c,cap}$ (±SE) of 20 ± 0.7 pS ($n = 30$). Interpolation (Fig. 6), gives an intracellular K^+ activity (K_{cell}) of 17 mM.

Collection of the data for Fig. 6 is rather time consuming. Therefore, it is important to note that once the value of K_s of a particular channel is known there is an alternative, faster way to calculate the intracellular ion activity. As is obvious from Eqs. 6 and 7, when using the ratio of two conductances and assuming that P_s is the

same under the two conditions, P_s cancels out of the equation. Suppose we already knew K_s, then it would suffice to determine the single-channel conductance and reversal potential of $I_{K,out}$, first in the CAP configuration and secondly in the IOP configuration, preferably on the same membrane patch. Then, the ratio of g_c in the CAP configuration ($g_{c,cap}$) and in the IOP configuration ($g_{c,iop}$) is given by:

$$\frac{g_{c,cap}}{g_{c,iop}} = \frac{(K_{cell}(K_p + K_s) + K_p(K_{cell} + K_s))(K_{b,iop} + K_s)(K_p + K_s)}{(K_{b,iop}(K_p + K_s) + K_p(K_{b,iop} + K_s))(K_{cell} + K_s)(K_p + K_s)} \quad (8)$$

where K_p is the pipette K^+ concentration (which is the same for a CAP and an IOP measurement on the same membrane patch) and $K_{b,iop}$ the bath K^+ concentration during the IOP recording. It is impossible to express K_{cell} explicitly in terms of known parameters and therefore we used an iterative calculation in PASCAL to solve Eq. 8 for K_{cell}. The $g_{c,iop}$ at a K^+ activity in the bath of, for instance, 86 mM, was observed to be 28 ± 0.6 pS ($n = 11$). And when using the above-mentioned $g_{c,cap}$ of 20 pS and K_s of 20 mM, we calculate a cytosolic K^+ activity of 18 mM, indeed almost identical to the 17 mM obtained by interpolation from Fig. 6.

Prior to the patch-clamp experiments, the cells were kept on ice in a standard solution containing less than 5 mM K^+. This may partly explain the low calculated K_{cell} (17 mM). One way to test the sensitivity of the method would be to load *Vicia faba* guard cells with K^+ and study the effect on $g_{c,cap}$. To induce K^+-uptake, we incubated the cells for at least two hours in a solution containing 50 mM KCl but recorded $g_{c,cap}$ and V_p^0 in a solution containing 11 mM K^+. Under these conditions, we indeed observed an increase in $g_{c,cap}$, from 20 pS to 25 ± 1.4 pS ($n = 5$). Again using Fig. 6, interpolation then yields a K_{cell} of 40 mM, indicating that the incubation in 50 mM KCl had indeed influenced the cytosolic K^+ concentration.

Calculation of the Membrane Potential

The next step is to calculate V_i, which, in the special case of $\delta = \beta \approx 0$, equals E_0 (Eq. 1). Then, according to Eq. 5, E_0 is given by the sum of V_p^0 and E_c:

$$E_0 = V_p^0 + E_c \quad (9)$$

Figure 7 shows V_p^0 at different K^+ activities in the bath. The solid line represents the theoretical value of V_p^0 for cells that occupy the ''K-state'' (Vogelzang & Prins, 1994), in which V_i is dominated by a K^+ conductance. For these cells V_p^0 is independent of K_{cell} and is solely defined by the pipette and bath solutions: $V_p^0 = (RT/F)\ln(K_{bath}/K_{pipette})$. The dotted lines in Fig. 7 mark the area of E_K ± 10 mV. Figure 7 shows that for the majority of cells (33 out of 54), V_p^0 was close to E_K,

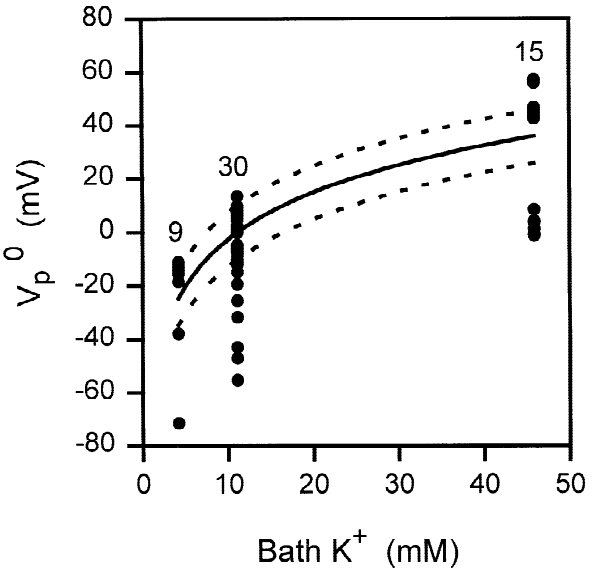

Fig. 7. Values of V_p^0 at different K^+ activities in the bath. Prior to the recordings, the cells were incubated in a low (<5 mM) K^+ solution. The K^+ activity in the pipette was always 11 mM. The solid line represents calculated E_K based on the K^+ activity in the pipette and the bath. The dashed lines mark E_K ± 10 mV. Numbers represent the number of independent experiments for each condition. K^+ activities given include the contribution of K^+ from KOH for pH adjustment.

indicating that these cells indeed occupied the K-state. Based on Fig. 7, at a bath K^+ activity of 11 mM, the average V_p^0 for cells in the K-state was (±SE) 5 ± 1.2 mV ($n = 12$).

The value of E_c in the CAP configuration can be obtained by making use of the fact that the channel shows a K^+ selectivity. Consequently, once we have calculated K_{cell}, E_c is simply given by the Nernst potential of K^+ (E_K):

$$E_{c,cap} = E_K = \frac{RT}{F} ln \frac{K_p}{K_{cell}} \quad (10)$$

resulting in an E_c of −11 mV and in an E_0 of −6 mV. Occasionally, however, V_p^0 was about 50 mV more negative than E_K, most likely reflecting activity of the outwardly directed, plasma membrane bound H^+-ATPase in these cells (Shimazaki, Iino & Zeiger, 1986).

After incubation in the 50 mM KCl solution, V_p^0 was 1 ± 0.9 mV ($n = 5$) and K_{cell} was 40 mM, resulting in an E_0 of −32 mV. The value of V_p^0 of 1 mV is close to the average V_p^0 of 5 mV measured under standard conditions at a bath K^+ of 11 mM and for cells in the K-state (*see* Fig. 7). This result is exactly as predicted for cells in the K-state and demonstrates the fact that under those conditions V_p^0 is indeed independent of K_{cell} (Vogelzang & Prins, 1994).

Discussion

Validity of the Method

The technique described here can be used for plant and animal cells and for plant vacuoles. Its application may be most biologically relevant for cells that face bulk flow of ions across their cell membrane as part of volume regulation, for instance epithelial cells in the kidney and the intestine and, in general, dividing cells (Jentsch & Günther, 1997). Among plant cells, the guard cell is probably the best example. We illustrated the method with recordings from inside-out patches but outside-out patches can be used as well.

The calculation of K_{cell} and V_i is most reliable when the channel studied is highly selective for one ion species and the cell size is relatively large and by implication $R_o \ll R_c$ and $R_o \ll R_p$. Then, effects of δ and β can simply be ignored. In the CAP configuration, the time constant of single channel current decay after a current transient depends on the relative values of both R_o and the intact cell capacitance. Therefore, a first look at the current traces can already reveal a coarse indication of the significance of R_o. Small values of R_o will result in rectangular shaped current pulses (e.g., Figs. 3*A* and 4*A*). In contrast, high values of R_o may result in decaying current pulses (Barry & Lynch, 1991; Ravesloot et al., 1994).

Obviously, one should be careful that during the CAP measurement the pipette is indeed attached to the cell and that the patch has not excised. In the case of $I_{K,out}$ in *Vicia faba* guard cells, confusion about the actual configuration was hardly possible as the channel consistently inactivated after excision, possibly due to the exposure of the channel to mM Ca^{2+} concentrations in the bath.

It should be stressed that the method relies on two presumptions. First, it is almost trivial to mention that one and the same channel should be studied in the CAP and excised patch configuration. For $I_{K,out}$ in *Vicia faba* guard cells the evidence was twofold. First, the similar voltage dependence and, second, the typical flickering, noisy open state current level observed in both configurations (Figs. 3*A* and 4*A*). Obviously, the likelihood that the same channel is studied increases significantly when both measurements are performed on one and the same membrane patch.

Second, a difference in channel conductance between the CAP and the IOP recording must not be explicable by a regulatory effect of, for instance, a cytosolic component that is present only during the CAP measurement. In this respect, knowledge of the physiology of the particular cell may be helpful. One may choose those experimental conditions which have a predictable effect on, for instance, cytosolic Ca^{2+} and pH. We can address this point with an example. We previously showed (Miedema & Assmann, 1996) that $I_{K,out}$ is affected by the cytosolic pH (pH_i). An increase of pH_i from 7 to 8 caused an 1.2-fold increase in g_c. Recordings on one and the same membrane patch revealed that the channel activity in CAP was most like the observed channel activity during the IOP measurement at a bath pH of 8. This observation suggests that under the given conditions, the pH_i of guard cell protoplasts is closer to 8 than to 7. Measurements on intact *Vicia faba* guard cells indeed indicate a somewhat alkaline pH_i of 7.7 (Blatt & Armstrong, 1993). Therefore, we compared the CAP measurements with IOP recordings obtained at a bath pH of 8. This may be an unusual case, since channel regulation is more commonly achieved by regulation of the open probability (P_o) rather than at the level of g_c. The effect of external K^+ on $I_{K,out}$ in *Vicia faba* guard cells can serve as a typical example. While the activation potential of $I_{K,out}$ shifts with E_K, the single channel conductance remains unaffected (Blatt & Gradmann, 1997 and references therein). Provided one is able to observe multiple channels during a CAP recording, a change in P_o does not affect our method.

It might be obvious that the method fails whenever V_i shows an unstable, drifing behavior. In general, membrane potentials dominated by diffusion potentials are more stable than membrane potentials dominated by electrogenic transporters. In this respect, the method might be more applicable to animal than plant systems, as the latter are more often hyperpolarized and (partly) defined by the plasma membrane bound H^+-ATPase. We observed such a drifting V_i (*data not shown*) after the addition to the guard cell protoplasts of fusicoccin, a compound known to stimulate the proton pump (Marrè, 1979).

Another limitation of the method arises from the fact that for some channels the concentration dependence of g_c may deviate significantly from the simple saturation curve shown in Fig. 6. For instance, for multi-ion pores, g_c may actually decrease at higher substrate concentration (Hille, 1992). Then, an interpolation as shown in Fig. 6 results in two possible solutions.

We concluded that our data are much better described by Eqs. 6 and 7 (Fig. 5*B*) than by the GHK equation (Fig. 5*A*). However, the opposite will be true for other types of channels. The use of the GHK equation has the advantage that the method does not rely on the knowledge of K_s and P_s, because the GHK equation contains only one parameter, P_s, which, when using current or conductance ratios, cancels out of the equation (*see* Appendix). This significantly simplifies the procedure, and is even more relevant when considering that, at least for our data, the variation in the final calculated value of K_{cell} was mainly determined by variation in the values of K_s and P_s as obtained from Fig. 6, rather than in the variation in $g_{c,cap}$.

Cytosolic K^+ and Membrane Potential in *Vicia faba* Guard Cells

From impalement studies on intact cells, *Vicia faba* guard cells can be divided into two subpopulations (Thiel, MacRobbie & Blatt, 1994). One group of cells is characterized by a membrane potential that shows a near-Nernstian behavior with extracellular K^+ (''K-state''). The membrane potential of cells of the second group is more negative than E_K, indicating a V_i dominated by the H^+-ATPase. Figure 7 supports this categorization of guard cells into ''K-state'' and ''pump-state'' cells. Recently, Roelfsema and Prins (1997) arrived at the same categorization from double–barreled voltage clamp measurements on guard cells in *Arabidopsis* epidermal peels.

Guard cells regulate stomatal aperture and guard cell swelling and shrinking is accomplished by the uptake or release of cations and anions, notably K^+, Cl^- and malate (Assmann, 1993). Consequently, the concentrations of these ions in guard cells may vary considerably, depending on the physiological status of the cell. This may be one explanation for the large variability in K^+ concentrations reported in the literature. Reported values range from 0–80 mM for isolated, 'closed' guard cell protoplasts to 276–357 mM for isolated, 'open' guard cell protoplasts. For intact cells, i.e., cells still situated in the epidermal strip, the estimates are 77–80 mM for 'closed' and 460–880 mM for 'open' guard cells (MacRobbie, 1988 and references therein). These measurements of cell K^+ are based on electron probe measurements, $^{42}K^+$ uptake experiments or the use of ion-selective microelectrodes. Considering the activity of 17 mM we found, it is suggested that the cells we used represented the closed state of the stomata (*see also* MacRobbie, 1986). This finding is in accordance with the low light intensity used during the experiments and the 0.5 mM Ca^{2+} in the bathing solution: both conditions are known to inhibit K^+ uptake and stomatal opening (Schwartz, Ilan & Grantz, 1988). This conclusion is also consistent with the observation that most of the cells were in the K-state, with little apparent pump activity: low light intensities and Ca^{2+} inhibit the H^+ ATPase of guard cells (Shimazaki et al., 1986; Kinoshita, Nishimura & Shimazaki, 1995), thereby maintaining stomata in the closed state.

A second reason for the large variability in reported K^+ concentrations is uncertainty about what the values actually represent: cytosolic, vacuolar or total K^+ concentration. The swelling of guard cells requires a significant uptake of water and thus of salt storage in the vacuole. However, to date it has been unknown whether this is accompanied by an increase of cytosolic ion concentrations as well. The method described here can address this question. From the K^+ uptake experiments described here, it is obvious that a high extracellular K^+ concentration (which induces stomatal opening (Schwartz et al., 1988)) can indeed induce a significant rise in cytosolic K^+ concentrations.

In general, impalement of plant cells with potential or ion selective electrodes is often inconclusive because of confusion regarding the exact location of the electrode tip, in the cytosol or in the vacuole. The use of ion selective fluorescent probes such as potassium or sodium binding benzofuran isophtalate (PBFI and SBFI) is complicated because these probes show a pH-and-ionic strength-dependent affinity for both K^+ and Na^+ (Haughland, 1996). The method outlined in this paper overcomes these problems and is noninvasive, providing an attractive alternative approach for the measurement of intracellular ion activities and membrane potential in both plant and animal cells.

We thank the scientists who commented on the manuscript, particularly Drs. F. Gómez-Lagunes and O. Pantoja. This research was supported by NSF grant MCB-9316319 to S.M. Assmann.

References

Assmann, S.M. 1993. Signal transduction in guard cells. *Annu. Rev. Cell Biol.* **9:**345–375

Barry, P.H., Lynch, J.W. 1991. Liquid junction potentials and small cell effects in patch-clamp analysis. *J. Membrane Biol.* **121:**101–117

Blatt, M.R., Armstrong, F. 1993. K^+ channels of stomatal guard cells: abscisic acid-evoked control of the outward rectifier mediated by cytoplasmic pH. *Planta* **191:**330–341

Blatt, M.R., Gradmann, D. 1997. K^+-sensitive gating of the K^+ outward rectifier in *Vicia* guard cells. *J. Membrane Biol.* **158:**241–256

Fischmeister, R., Ayer, R.K., DeHaan, R.L. 1986. Some limitations of the cell-attached patch clamp technique: a two-electrode analysis. *Pfluegers Arch.* **406:**73–82

Haughland, R.P. 1996. Handbook of Fluorescent Probes and Research Chemicals. Molecular Probes, Eugene, OR

Hille, B. 1992. Ionic Channels of Excitable Membranes. Sinauer Associates, Sunderland, MA

Jentsch, T.J., Gunther, W. 1997. Chloride channels: an emerging molecular picture. *BioEssays* **19:**117–126

Kinoshita, T., Nishimura, M., Shimazaki, K. 1995. Cytosolic concentration of Ca^{2+} regulates the plasma membrane H^+-ATPase in guard cells of fava bean. *Plant Cell* **7:**1333–1342

Lynch, J.W., Barry, P.H. 1989. Action potentials initiated by single channels opening in a small neuron (rat olfactory receptor). *Biophys. J.* **55:**755–768

MacRobbie, E.A.C. 1988. Control of ion fluxes in stomatal guard cells. *Botanica Acta* **101:**140–148

Marrè, E. 1979. Fusicoccin: a tool in plant physiology. *Annu. Rev. Plant Physiol.* **30:**273–288

Miedema, H., Assmann, S.H. 1996. A membrane-delimited effect of internal pH on the K^+ outward rectifier of *Vicia faba* guard cells. *J. Membrane Biol.* **154:**227–237

Offner, F.F. 1991. Ion flow through membranes and the resting potential of cells. *J. Membrane Biol.* **123:**171–182

Ravesloot, J.H., Van Putten, M.J.A.M., Jalink, K., Ypey, D.L. 1994. Analysis of decaying unitary currents in on-cell patches of cells with a high membrane resistance. *Am. J. Physiol.* **266:**C853–C869

Roelfsema, M.R.G., Prins, H.B.A. 1997. Ion channels in guard cells of *Arabidopsis thaliana* (L.) Heynh. *Planta* **202:**18–27

Schwartz, A., Ilan, N., Grantz, D.A. 1988. Calcium effects on stomatal movements in *Commelina communis* L. *Plant Physiol.* **87:**583–587

Shimazaki, K-I., Iino, M., Zeiger, E. 1986. Blue light-dependent proton extrusion by guard cell protoplasts of *Vicia faba. Nature* **319:**324–326

Thiel, G., MacRobbie, E.A.C., Blatt, M.R. 1992. Membrane transport in stomatal guard cells: the importance of voltage control. *J. Membrane Biol.* **126:**1–18

Vogelzang, S.A., Prins, H.B.A. 1994. Patch-clamp analysis of the dominant plasma membrane K^+ channel in root cell protoplasts of *Plantago media* L. Its significance for the P and K-state. *J. Membrane Biol.* **141:**113–122

Appendix

Because the behavior of many channel types will be best fitted by the GHK equation rather than by Offner's equation, in this section we outline our method with the use of the GHK equation. We will demonstrate the calculation by using current or conductance ratios rather than using an interpolation as shown in Fig. 6. We will only discuss the special case in which $\delta = \beta \approx 0$. Under the constraint of independent ion movement, the GHK equation provides a quantitative description of the relationship between the ionic current (I_s), the electrical potential across the membrane (E) and the internal and external ion activities, S_i and S_o, respectively:

$$I_s = P_s z_s^2 \frac{EF^2}{RT} \frac{S_i - S_o \exp(-z_s v)}{1 - \exp(-z_s v)} \tag{11}$$

where z_s is the valence of the ion species and v equals FE/RT where R, T and F have their usual meaning. As is true for Eq. 7, the application of Eq. 11 requires the knowledge of the absolute value of P_s. However, when comparing the ratio of currents (I'/I) as measured under two different ionic conditions while assuming that P_s remains unaffected, P_s cancels out of the equation:

$$\frac{I'}{I} = \frac{E'(S_{i'} - S_{o'} \exp(-z_s v'))(1 - \exp(-z_s v))}{E(S_i - S_o \exp(-z_s v))(1 - \exp(-z_s v'))} \tag{12}$$

Note that in the case where the electrical potential across the membrane is identical under the two different conditions ($E = E'$), for example during two measurements on an excised patch, Eq. 12 is simplified to Eq. 13 (*see* Eq. 14-3 in Hille, 1992):

$$\frac{I'}{I} = \frac{S_{i'} - S_{o'} \exp(-z_s v')}{S_i - S_o \exp(-z_s v)} \tag{13}$$

In the case where g_c and $g_{c,cap}$ show ohmic behavior, instead of using current magnitudes we can introduce g_c in Eq. 13 by calculating I from Eq. 6.

As an example, suppose we consider K^+ currents obtained from CAP and IOP recordings. Then, according to Eq. 12 the ratio of g_c in the CAP and the IOP configuration ($g_{c,cap}/g_{c,iop}$) equals:

$$\frac{g_{c,cap}}{g_{c,iop}} = \frac{A}{B} C \tag{14}$$

where

$$A = E_{cap} \frac{(K_{cell} - K_p \exp(-v))_{cap}}{1 - \exp(-v)_{cap}} \tag{15}$$

$$B = E_{iop} \frac{(K_b - K_p \exp(-v))_{iop}}{1 - \exp(-v)_{iop}} \tag{16}$$

$$C = \frac{(E - E_c)_{iop}}{(E - E_c)_{cap}} \tag{17}$$

where K_b is the K^+ concentration in the bath during the IOP recording and K_p is the K^+ concentration in the pipette.

In the CAP configuration, the actual potential across the membrane patch (E_{cap}) is given by:

$$E_{cap} = V_i - E_c - V_p \tag{A6, 18}$$

Given that $\delta = \beta \approx 0$, V_i equals E_0 (Eq. 1) and E_c equals $E_0 - V_p^0$ (Eq. 5). Consequently, E_{cap} equals $V_p^0 - V_p$. Replacing $E_{c,cap}$ in Eq. 17 with Eq. 10 and using $E_{iop} = -V_p$, finally results in an expression with K_{cell} as the only unknown parameter. This expression can be solved for K_{cell} iteratively in the manner explained before.

Whether Offner's equation or the GHK equation is used, a prerequisite for the calculation of the intracellular ion concentration as shown in this paper is that the particular conductance shows ohmic behavior. It should be stressed that the GHK equation predicts rather nonlinear behavior, especially in the case of a significant ion gradient across the membrane. This implies a limitation for the use of our technique if channel behavior, particularly under asymmetrical ionic conditions, is best described by the GHK equation.